

## GEMS-like material from asteroid Ryugu regolith

Hope A. Ishii<sup>1</sup>, John P. Bradley<sup>1</sup>, Elena Dobrică<sup>1</sup>, Kenta Ohtaki<sup>1</sup>, Takaaki Noguchi<sup>2,3</sup>, Toru Matsumoto<sup>4</sup>, the Min-Pet Fine Subteam and the Hayabusa2 initial analysis core

<sup>1</sup>*Hawai'i Institute of Geophysics and Planetology, University of Hawai'i at Mānoa, Honolulu, HI 96822, USA*

<sup>2</sup>*Division of Earth & Planetary Science, Kyoto University, Kyoto, Japan*

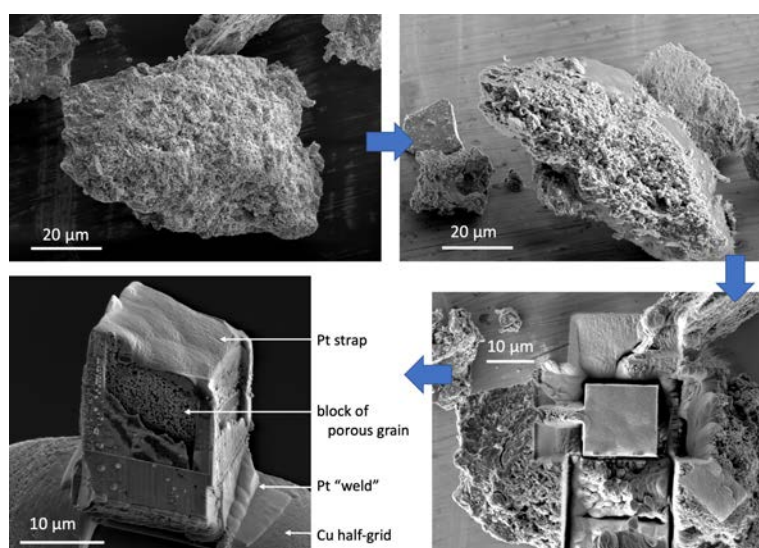
<sup>3</sup>*Department of Geology and Mineralogy, Kyushu University, Kyoto, Japan*

<sup>4</sup>*Hakubi Center for Advanced Research, Kyoto University, Kyoto, Japan*

**Introduction:** Because GEMS, glass with embedded metal (kamacite) and sulfides (pyrrhotite) are found in primitive cometary particles and likely accreted at extremely low temperatures, their presence is often taken as an indicator of cosmic primitivity and lack of alteration in meteoritic parent bodies [1]. GEMS are found in anhydrous, carbon-rich interplanetary dust particles (IDPs) and have also been confirmed in Antarctic micrometeorites (MMs) [2]. GEMS-like materials, having similar texture and morphology (glass with embedded opaques) have been reported in several chondrites, e.g. [3,4]. Close study in some chondrites shows key differences to GEMS in cometary-type particles, for example, in size range, glassy matrix composition and mineralogy of opaques [5,6]. JAXA's Hayabusa2 mission returned regolith from near-Earth Cb-type asteroid 162173 Ryugu, and GEMS-like material has recently been reported in Ryugu regolith grains within less-altered lithologies [7].

**Samples and Methods:** Two Ryugu grains with high porosity, A0104-029025 and C0105-039023, were identified late in the initial analysis period and analyzed to determine if they contain GEMS. Initial characterization was performed by scanning electron microscopy (SEM) and energy dispersive X-ray spectroscopy (EDS) on a JEOL JSM-7001F FE-SEM at Kyoto U. a ThermoFisher Scios FIB-SEM at Kyushu U., and a ThermoFisher Helios Nanolab 660 FIB-SEM at U. Hawaii. SEM-EDS characterization shows that grain A0104-029025 is ~50  $\mu\text{m}$  in length and has a silica-rich matrix holding remnant olivine up to ~5  $\mu\text{m}$  across, pyrrhotite, pentlandite, magnetite, Mg-rich Cr-spinel, calcite, and a Fe-Ni-P-bearing phase. Grain C0105-039023 is ~75  $\mu\text{m}$  in length and its silica-rich matrix contains smaller remnant olivine and pyroxene grains, pyrrhotite, pentlandite, magnetite, Cr-spinel, dolomite, calcite, phosphates, and a submicron-sized fragment of the Ta projectile. Using Focused Ion Beam (FIB) methods, regions of both samples were extracted as blocks (e.g., Fig. 1), embedded in epoxy, and ultramicrotomed to produce electron-transparent sections for analysis by scanning transmission electron microscopy (STEM). STEM analyses were performed using a ThermoFisher TitanX 60-300 with 4-quadrant windowless EDS detector at the Molecular Foundry, Lawrence Berkeley National Laboratory.

Figure 1. Preparation of FIB-extracted block from grain C0105-039023. Clockwise from top left: SE image of grain; view with sample tilted and protective Pt layer deposited; FIB milling to free block from grain; and final block mounted on a Cu TEM half-grid, ready for embedding and ultramicrotomy [after 8].



**Results:** Observed at modest TEM magnifications, C0105-039023 and A0104-029025 both contain regions of abundant fine-grained layer silicate with Fe-rich inclusions that has a GEMS-like appearance. Anhydrous silicates were not observed in either of the FIB-sections analyzed, although they were observed by SEM. C0105-039023 is dominated by compact, well-ordered layer silicates and with abundant pentlandite and pyrrhotite, minor Fe-oxides, and Mg,Ca-rich carbonates. High porosity in this grain is due to many cracks in the interior. Some GEMS-like objects with rounded shapes were identified in C0105-039023. Closer investigations revealed that, unlike in GEMS in cometary-type interplanetary dust particles and Antarctic micrometeorites, ultra-fine-grained inclusions are absent; no kamacite was detected; both pyrrhotite and pentlandite are present; and the "matrix" is layer silicate. We found that even in regions of the samples where imaging contrast appears uniform and suggestive of amorphous structure, poorly ordered fine fibers of layer silicate, a few basal spacings thick, are observed at high magnifications. Figure 2 shows a

few GEMS-like objects in C0105-039023. Compositions of these GEMS-like objects are approximately chondritic in major elements, like GEMS and other primitive objects. Higher carbon content in one GEMS-like object, relative to the surrounding matrix, is somewhat suggestive of *bona fide* GEMS that might have altered in place. The presence of co-located Na and Cl, presumably salt, in the same field of view as the GEMS-like objects underscores the significant role of aqueous processing in these grains.

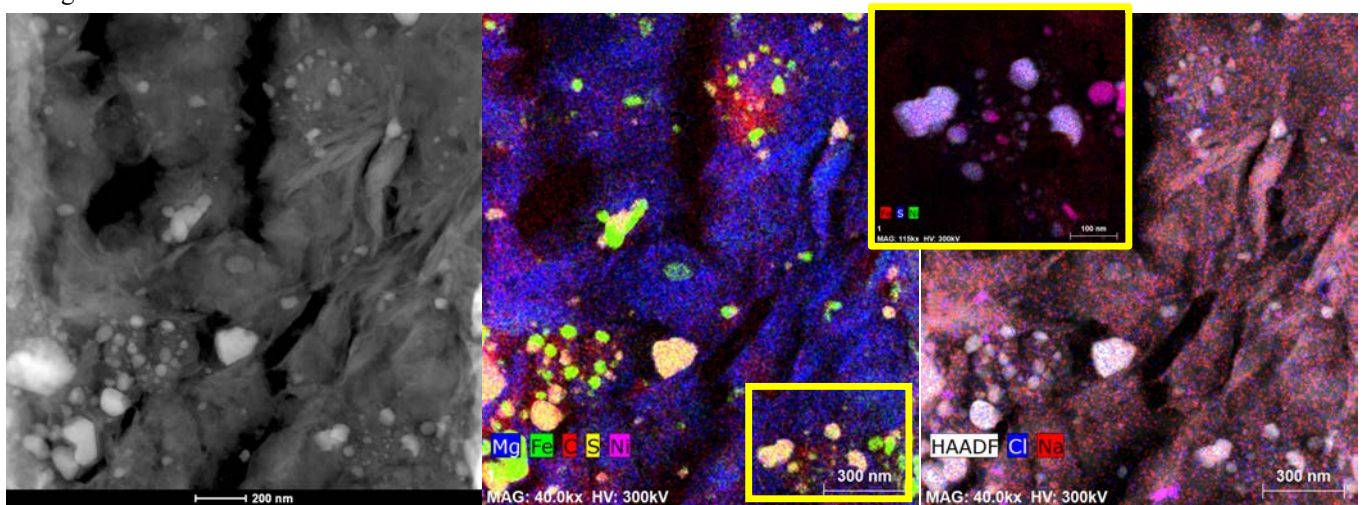


Figure 2. GEMS-like objects in Ryugu grain C0105-039023. Left: HAADF STEM image showing 3 GEMS-like objects located in upper right, lower right and lower left quadrants of image. Middle: EDS map of Mg (blue), Fe (green), C (red), S (yellow), Ni (magenta) of same region. One GEMS-like object is outlined in yellow and shown at higher magnification in an overlaid EDS map of Fe (red), S (blue) and Ni (green) showing presence of both pentlandite and pyrrhotite. The top right GEMS-like object has higher carbon content than surrounding layer silicate matrix. Right: HAADF STEM image overlaid by Cl (blue) and Na (red) EDS maps showing presence of NaCl (bottom, middle), indicative of aqueous processing.

A0104-029025 has two texturally distinct regions, one with high porosity and the other with lower porosity. The more porous region consists of poorly ordered, hydrated silicate and fine-grained pyrrhotite. Pentlandite was not observed in the high porosity region. The less porous region contains finer-grained pyrrhotite, pentlandite, and a platy S-rich phase thought to be proto-tochilinite. These mineralogical differences are evident in EDS maps over the boundary. No metal was observed in either of these two grains.

**Discussion and Conclusions:** Based on our observations, GEMS-like objects in porous Ryugu grains are not GEMS, as defined according to their characteristics in cometary-type IDPs and MMs. We observed one GEMS-like object with higher carbon content than its surroundings, suggestive of possible alteration in place of GEMS; however, the majority of GEMS-like objects contain pentlandite and pyrrhotite, no kamacite (metal) and have matrices that consist of poorly ordered hydrated silicate. Instead, we conclude that the GEMS-like objects in the porous Ryugu grains we studied are sulfide clusters that co-deposited with hydrated silicate. This interpretation of a likely role of aqueous processing is supported by the presence of NaCl near the GEMS-like objects in C0105-039023. For A0104-029025, we hypothesize that the observed boundary between high and lower porosities represents a leach front. The lower porosity region shows evidence of more extensive aqueous alteration in the form of pentlandite, reduced pyrrhotite grain size, and the platy sulfide that may result from oxidation of pyrrhotite. The observation of anhydrous silicates by FE-SEM demonstrates that aqueous alteration is incomplete, and larger anhydrous silicates in A0104-029025 support less heavy modification of that grain relative to C0105-039023. High porosity in both grains may reflect a sufficiently low degree of compaction and remnant porosity to allow aqueous alteration products to form in void spaces.

## References

- [1] Ishii H.A. et al. (2018) *Proc. National Academy Sci.* 115:6608-6613. [2] Noguchi T. et al. (2015) *Earth Planet. Sci. Lett.* 410:1-11. [3] Leroux H. et al (2015) *Geochimica et Cosmochimica Acta* 170:247-265. [4] Nittler L. R. et al. (2019) *Nature Astronomy* 3:659-666. [5] Ohtaki K. et al. (2021) *Geochimica et Cosmochimica Acta* 310:320-345. [6] Villalon K. R. et al. (2021) *ibid*, 346-362. [7] oral presentation, Nakamura T. et al. (2022) *LPS LIII*, Abstract #1753. [8] Ohtaki K. et al. (2020) *Microscopy & Microanalysis* 26:120-125.